D. (1979) *Biochemistry 18*, 780–790.
Poste, G., & Nicolson, G. L., Eds. (1978) *Cell Surf. Rev. 5*, 1–862.
Snyder, B., & Freire, E. (1980) *Proc. Natl. Acad. Sci. U.S.A. 77*, 4055–4059.
Struck, D. K., Hoekstra, D., & Pagano, R. E. (1981) *Biochemistry 20*, 4093–4099.
Vanderwerf, P., & Ullman, E. F. (1980) *Biochim. Biophys. Acta 596*, 302–314.
Van Dijck, P. W. M. (1979) *Biochim. Biophys. Acta 555*, 89–101.
Van Dijck, P. W. M., de Kruijff, B., Verkleij, A. J., Van Deenen, L. L. M., & de Gier, J. (1978) *Biochim. Biophys. Acta 512*, 84–96.
Wilschut, J., Duzgunes, N., Fraley, R., & Papahadjopoulos, D. (1980) *Biochemistry 19*, 6011–6021.
Wu, E., Jacobson, K., & Papahadjopoulos, D. (1977) *Biochemistry 16*, 3936–3941.

Structure and Thermotropic Behavior of Phosphatidylserine Bilayer Membranes†

Helmut Hauser, Fritz Paltauf, and G. Graham Shipley*

ABSTRACT: The structure and thermotropic properties of a homologous series of diacylphosphatidylserines (PS) in the anhydrous and hydrated state have been examined with low-angle X-ray diffraction and differential scanning calorimetry. In the anhydrous state at low temperatures both acidic PS and its NH_4^+ salts exhibit lamellar bilayer crystal forms that transform to liquid-crystalline hexagonal (type II) structures at higher temperatures. The crystal → liquid-crystal transition temperature increases with increasing chain length, the transition temperature of an NH_4^+-PS being higher than that of its corresponding acidic form. In contrast, the transition enthalpies of the acidic PS are higher than those of the NH_4^+ salt forms. Hydrated acidic PS and NH_4^+-PS exhibit reversible lamellar gel → liquid-crystal transitions. In this case the acidic form undergoes this chain length dependent transition at a higher temperature, but with a lower enthalpy change, than the NH_4^+-PS. Both below and above the hydrocarbon chain melting transition, hydrated lamellar bilayer structures are present. The temperature–composition phase diagram of the NH_4^+-dimyristoyl-PS/H_2O system has been studied in detail. The chain melting transition decreases with increasing hydration, reaching a limiting value of 39 °C. X-ray diffraction shows that both the bilayer gel structure and the bilayer liquid-crystal form take up water continuously (i.e., no hydration limit), a characteristic of lipid bilayers with a net charge. Electron-density profiles of NH_4^+-dimyristoyl-PS at different hydration levels permit detailed analysis of the structural parameters of the PS bilayer.

The structure and properties of uncharged zwitterionic membrane phospholipids, notably phosphatidylcholine and phosphatidylethanolamine, have been studied with a wide range of physical–chemical techniques. This approach has provided detailed information on their molecular conformation, bilayer-forming properties, and order–disorder thermotropic transitions, which, in turn, has led to a better understanding of their structural role in model and natural cell membranes [for reviews, see Shipley (1973) and Hauser et al. (1981)]. This approach has benefited greatly by the study of synthetic phospholipids in which the fatty acyl chain length and/or degree of unsaturation are systematically varied. In contrast, anionic membrane lipids such as phosphatidylserine (PS),[1] phosphatidylglycerol, and cardiolipin have received much less attention, and precise details of their structure and properties are lacking.

Phosphatidylserine is found in significant amounts in a wide variety of animal and bacterial cell membranes. In red blood cells it appears to be located mainly on the cytoplasmic side of the membrane. Physical–chemical studies of PS have been concerned primarily with the behavior of natural, mixed fatty acid PS, isolated usually from bovine brain. Bovine brain PS has been shown by X-ray diffraction and electron microscopy to form bilayer structures (Atkinson et al., 1974), and its structure and hydration were shown to be clearly dependent on its ionic environment (Hauser & Phillips, 1979). The structure and thermotropic properties of bovine brain PS have been shown to be sensitive to the presence of divalent cations Ca^{2+} and Mg^{2+}, and these studies have suggested that cation–PS complexes may be involved in membrane fusion processes (Papahadjopoulos et al., 1977). More recently, studies of synthetic PS with controlled fatty acid chain length have been reported (MacDonald et al., 1976; Luna & McConnell, 1977; van Dijck et al., 1978; van Dijck, 1979; Browning & Seelig, 1980). For example, DPPS has been shown to undergo a thermotropic transition at ~53 °C, utilizing differential scanning calorimetry (MacDonald et al., 1976; van Dijck,

† From the Departments of Medicine and Biochemistry, Biophysics Institute, Boston University School of Medicine, Boston, Massachusetts 02118 (G.G.S.), the Laboratorium für Biochemie, Eidgenossische Technische Hochschule Zurich, CH-8092 Zurich, Switzerland (H.H.), and the Institut für Biochemie, Technische Hochschule Graz, Graz, Austria (F.P.). *Received July 10, 1981.* This research was supported by grants from the U.S. Public Health Service (HL-26335) and the Swiss National Science Foundation (3.570-0.79). H.H. acknowledges receipt of a long-term fellowship from the European Molecular Biology Organization.

[1] Abbreviations: PS, phosphatidylserine; DDPS, didecanoylphosphatidylserine; DLPS, dilauroylphosphatidylserine; DMPS, dimyristoylphosphatidylserine; DPPS, dipalmitoylphosphatidylserine; DSPS, distearoylphosphatidylserine; DL-DLPS, dilauroylphosphatidylserine with glycerol C-2 in the racemic form; DL-DPPS, dipalmitoylphosphatidylserine with glycerol C-2 in the racemic form; DSC, differential scanning calorimetry; TLC, thin-layer chromatography. Unless stated otherwise, the glycerol is in the native D configuration and the serine in the native L form.

0006-2960/82/0421-1061$01.25/0

1979; Browning & Seelig, 1980), spin-label partitioning (Luna & McConnell, 1977), and ^{31}P and ^{2}H nuclear magnetic resonance (Browning & Seelig, 1980). These studies have led to an improved understanding of the conformation and properties of PS but have not yet provided details of its bilayer structure or the influence of ions on this structure.

In this paper, we describe the structure and thermotropic properties of the acidic and NH_4^+ salt forms of synthetic di-$C_{12:0}$-, di-$C_{14:0}$-, di-$C_{16:0}$-, and di-$C_{18:0}$-phosphatidylserines in both the anhydrous and hydrated state. These studies using X-ray diffraction and differential scanning calorimetry (DSC) form the basis for systematic studies of the effects of monovalent and divalent cations on PS (H. Hauser and G. G. Shipley, unpublished experiments).

Materials and Methods

A homologous series of 2,3-diacyl-D-glycero-1-phospho-L-serine and 2,3-diacyl-DL-glycero-1-phospho-L-serine compounds [for a discussion of the chemical nomenclature used, see Hauser et al. (1981)] were synthesized as described elsewhere (A. Hermetter, F. Paltauf, and H. Hauser, unpublished results). DMPS, DPPS, and DSPS were also synthesized by R. Berchtold (Biochemisches Labor, Berne) essentially according to the method of Aneja et al. (1970). The final product was phosphatidylserine in either the acidic or NH_4^+ salt form. Serine was always present in the native L form, and, unless stated otherwise, the optically active form of glycerol was used with the C-2 in the native D configuration. The purity of the lipids was monitored by thin-layer chromatography (TLC) on 20 cm × 20 cm silica gel 60 F-254 plates (Merck, AG), with two solvent systems ($CHCl_3/CH_3OH/NH_3$, 65:25:4 v/v; $CHCl_3/CH_3OH$/acetic acid/H_2O, 50:30:8:4 v/v). Lipids were detected (1) by exposing the TLC plate to iodine, (2) by spraying with molybdenum blue spray (Applied Science, State College, PA), (3) by spraying with 0.1 M ninhydrin in 2-propanol, and (4) by exposing to 50% sulfuric acid followed by charring. Small amounts of degradation products, which formed during storage or as a result of sample handling, were removed by column chromatography on silicic acid or by preparative TLC with silica gel H plates, 20 cm × 20 cm, 0.25-mm thickness (Analtech). The plates were washed with $CHCl_3/CH_3OH$/diethyl ether, 1:1:1 (v/v), and activated at 110 °C before use. The same solvents as described above were used. The lipid bands were made visible by short exposure of the plates to iodine vapor, scraping off the silica gel containing the lipid, and eluting the lipid with $CHCl_3/CH_3OH$/diethyl ether, 1:1:1 (v/v), according to Kates (1975). For conversion of the acid form into the ammonium salt, the acid was dissolved in sufficient $CHCl_3/CH_3OH/NH_3$, 60:35:5 (v/v); undissolved material was removed by filtering through a glass-sintered disk, and the filtrate was taken to dryness on the rotary evaporator at a temperature below 30 °C. The dry residue was dispersed in acetone and the dispersion filtered through a glass-sintered disk. The residue on the filter was thoroughly washed with acetone and dried over potassium hydroxide in vacuo. The yield of the ammonium salt was 80%. Sometimes, the NH_4^+ salt of phosphatidylserine was converted to the acidic form by dissolving the lipid in $CHCl_3/CH_3OH$, 1:1 (v/v), and adding 0.45 volume of 0.5 M HCl. The upper phase was removed by suction and the lower $CHCl_3$-rich phase washed repeatedly with 0.2 volume of 0.5 M HCl.

Sample Preparation. For scanning calorimetry of anhydrous PS, a $CHCl_3/CH_3OH$, 2:1 (v/v), solution of the lipid was injected into a stainless steel DSC pan, and after evaporation of the solvent the lipid was dried to constant weight. For hydrated samples the solid material (1–5 mg) was weighed into the DSC pan and the appropriate amount of aqueous solvent added gravimetrically. The DSC pan was immediately sealed and transferred to the differential scanning calorimeter. For X-ray diffraction studies of anhydrous PS, the lipids were crystallized from $CHCl_3/CH_3OH$, 2:1 (v/v), and the polycrystalline sample was sealed into a thin-walled glass capillary tube (internal diameter 1 mm).

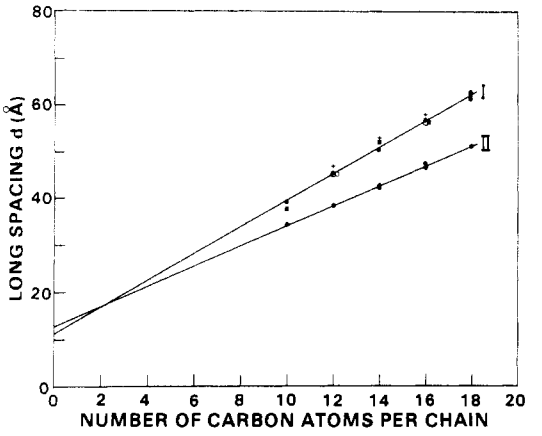

FIGURE 1: X-ray diffraction long spacings of the two forms of anhydrous phosphatidylserines as a function of hydrocarbon chain length: (●) acidic PS (D, L); (○) acidic PS (DL, L); (+) K^+-PS (D, L); (■) NH_4^+-PS (D, L); (□) NH_4^+-PS (DL, L).

Hydrated samples were prepared by weighing a known amount of the lipid into a glass tube with a narrow constriction in the center. After addition of the appropriate amount of water or salt solution by weighing, the glass tube was immediately sealed and the lipid dispersion homogenized by centrifuging it through the constriction repeatedly (6–12 times) at a temperature above the chain melting transition. The accuracy in the determination of the water content was better than ±5% in the 50% water region. Samples prepared in this manner were examined by both X-ray diffraction and DSC.

Methods. The calorimetric studies were performed with a Perkin-Elmer (Norwalk, CT) DSC-2 differential scanning calorimeter. Each sample was heated and cooled repeatedly, usually at a rate of 5 °C/min. The peak in the heat capacity vs. temperature plot was taken as the transition temperature, T_c; transition enthalpies were determined from the area under the peak as measured by planimetry and compared with the known enthalpy of a standard (gallium).

For X-ray diffraction studies, nickel-filtered Cu Kα X-radiation from an Elliott GX-6 rotating anode generator (Elliott Automation, Borehamwood, England) was used. The X-rays were focused by using a camera with toroidal optics (Elliott, 1965), and the X-ray diffraction patterns were recorded from samples maintained at different temperatures with a variable-temperature specimen holder. X-ray diffraction intensities were derived with a Joyce-Loebl Model III-CS microdensiometer. For more details of the method, see Janiak et al. (1976).

Results

Anhydrous Phosphatidylserine. X-ray diffraction of various preparations of anhydrous phosphatidylserine shows evidence of polymorphism. At room temperature, the long spacing *d*, representing the bilayer periodicity of the acidic form of D- and DL-PS, is linearly dependent on the fatty acid chain length for the even numbers of the homologous series (crystal form I in Figure 1). This form is characterized by a diffraction pattern in which the sharp low-angle diffraction lines are in a ratio 1:(1/2):(1/3):(1/4) ... indicating a lamellar bilayer

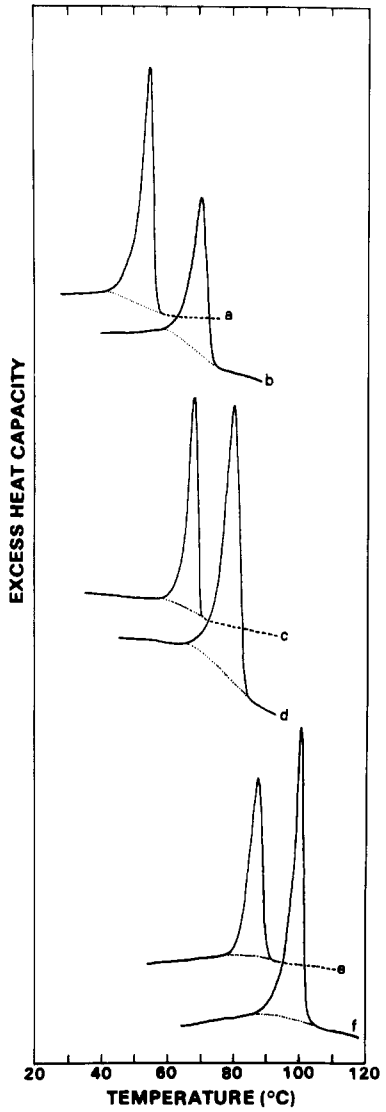

FIGURE 2: DSC thermograms of anhydrous diacylphosphatidylserines. Heating curves recorded at 5 °C/min are shown for (a) acidic DMPS, (b) NH_4^+-DMPS, (c) acidic DPPS, (d) NH_4^+-DPPS, (e) acidic DSPS, and (f) NH_4^+-DSPS.

structure. The linear relationship between long spacing and hydrocarbon chain length for this form with an increment of 2.52 Å/CH_2 group suggests that the orientation of the hydrocarbon chains is approximately normal to the layer plane. The extrapolated *d* value to zero chain length suggests that the two polar groups contribute approximately 12 Å to the bilayer periodicity, i.e., 6 Å/glycerophosphorylserine group. As indicated in Figure 1, *d* values for the corresponding anhydrous NH_4^+ and K^+ salts of PS lie close to this line for crystal form I and would suggest similar packing arrangements and lack of hydrocarbon chain tilting with respect to the normal to the bilayer plane. Under some conditions, the D form of acidic PS can crystallize into a different crystal form, and a different molecular packing and chain tilting are suggested (crystal form II in Figure 1). As an example of the complex polymorphic behavior of acidic phosphatidylserine, anhydrous acidic DPPS crystallizes from chloroform/methanol (2:1 v/v) solution into crystal form II with a lamellar periodicity d = 46.4 Å. Heating to 125 °C and cooling to 30 °C produce crystal form I with a lamellar periodicity d = 55.5 Å. On heating crystal form I through the endothermic transition at 68 °C (see below, Figure 2, and Table I), the low-angle diffraction pattern consists of two reflections at d = 35.3 and 20.5 Å. These reflections index according to 10 and 11

Table I: Transition Temperatures (T_c), Enthalpies (ΔH), and Entropies (ΔS) of Anhydrous Diacyl-PS

PS	T_c (°C)	ΔH (kcal/mol)	ΔS [cal/(mol·K)]
NH_4^+-DL-DLPS	56.5	3.4	10.3
acidic DMPS	54.5	9.5	29.1
NH_4^+-DMPS	70.0	5.4	15.6
acidic DPPS	68.0	11.3	33.2
acidic DL-DPPS	67.0	9.5	27.9
NH_4^+-DPPS	80.0	6.4	18.1
acidic DSPS	86.0	13.2	36.8
NH_4^+-DSPS	99.0	11.1	29.8

Table II: Transition Temperatures (T_c), Enthalpies (ΔH), and Entropies (ΔS) of Fully Hydrated Diacyl-PS

PS	T_c (°C)	ΔH (kcal/mol)	ΔS [cal/(mol·K)]
acidic DL-DLPS	32.5	3.1	10.1
NH_4^+-DL-DLPS	17.0	4.9	16.9
acidic DMPS	52.0	5.3	16.3
NH_4^+-DMPS	39.0	7.4	23.7
acidic DPPS	67.0	8.1	23.8
NH_4^+-DPPS	54.0	9.1	27.8
acidic DSPS	79.0	10.2	29.0
NH_4^+-DSPS	70.0	11.0	32.1

reflections of a hexagonal lattice, and it seems probable that the liquid-crystalline phase of the acidic PS is hexagonal type II [for the nomenclature and description of these phases, see Luzzati (1968) and Shipley (1973)].

This complex polymorphic behavior is evident in the scanning calorimetry studies of anhydrous PS. The initial heating from 0 °C gives a large enthalpy transition which shows no well-defined dependence on chain length for either the acidic or NH_4^+ salt forms of PS. On cooling, an exothermic transition is observed at lower temperature. For all anhydrous PS samples the second heating run exhibits an endothermic transition at a lower temperature than that observed on initial heating, and, as shown in Figure 2, the transition temperature shows a rational dependence on hydrocarbon chain length for both the acidic and NH_4^+ salt forms. This transition is reversible and repeated heating and cooling cycles show essentially the same behavior. For a given chain length, the NH_4^+ salt undergoes the order–disorder transition at a temperature 12–16 °C higher than that of the corresponding acidic PS. However, the transition enthalpy of the acidic form is higher than that of the NH_4^+ salt form (see Table I). For both acidic and NH_4^+ salt PS, increasing the chain length results in an increase in both the transition temperature and transition enthalpy (Figure 2 and Table I). Similar thermal behavior is observed for the natural D form of DPPS and its racemic DL counterpart (Table I).

Hydrated Phosphatidylserine. Differential scanning calorimetry heating curves of fully hydrated diacyl-PS (3–20 wt %) are shown in Figure 3. Both the acidic and NH_4^+ salt forms show fairly sharp reversible transitions. However, in contrast to the anhydrous state (see above), the transition temperature of the NH_4^+-PS in the hydrated state is 10–15 °C lower than that of the acidic form. The acidic PS give consistently lower transition enthalpies than the corresponding NH_4^+ salts (Table II). Again, increasing the chain length results in an increase in both transition temperature and transition enthalpy for the acidic and NH_4^+ salt series (Table II). The transition temperatures of both acidic PS and NH_4^+-PS appear to show a curvilinear dependence on chain length as shown in Figure 4. Alterations in the buffer concentration have a small effect on the transition temperature

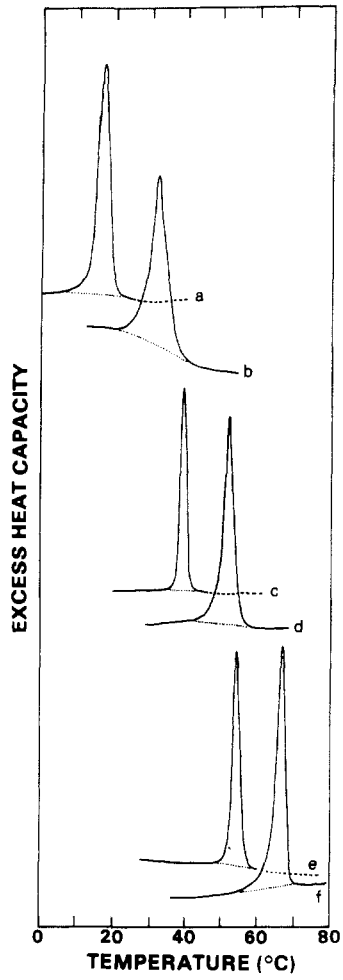

FIGURE 3: DSC thermograms of fully hydrated phosphatidylserines. Heating curves recorded at 5 °C/min are shown for (a) NH_4^+-DL-DLPS, (b) acidic DL-DLPS, (c) NH_4^+-DMPS, (d) acidic DMPS, (e) NH_4^+-DPPS, and (f) acidic DPPS. The NH_4^+ salts were dispersed in 0.025 M ammonium phosphate buffer (pH 6.8, I = 0.05); the acid forms were dispersed in 0.01 M HCl. Upon cooling, single sharp transitions occur with the transition temperature depressed by 3–6 °C compared to the transition temperature on heating. Both the endothermic and exothermic transitions were reproducible on successive heating and cooling cycles, respectively.

of the NH_4^+ salts, and small differences are observed at higher NH_4^+-PS concentrations (50 wt %), as shown in Figure 4 (dashed line).

For the NH_4^+-PS of different chain length, 50 wt % water dispersions were prepared and examined by X-ray diffraction at temperatures below and above their respective transition temperatures. With the exception of NH_4^+-DSPS above its transition temperature (see below), all samples give low-angle diffraction lines in the ratio 1:(1/2):(1/3):(1/4) ... characteristic of a lamellar bilayer phase. Below the transition, a single sharp reflection at 1/4.2 $Å^{-1}$ is observed, indicating the presence of a hydrated gel phase. Above the transition temperature a single broad reflection at 1/4.6 $Å^{-1}$ indicative of the "melted chain" liquid-crystal phase is observed. In spite of the fact that the X-ray data are not recorded at either a fixed temperature above or below the transition or at a specific "reduced" temperature with respect to the transition temperature, the bilayer repeat distance vs. the PS hydrocarbon chain length shows a linear relationship for both the gel and liquid-crystal bilayers (Figure 5). A linear-regression analysis was applied to the data to derive the repeat distance, d, at zero chain length. The values obtained are 67 Å for PS below the gel → liquid-crystal transition and 51 Å above the transition.

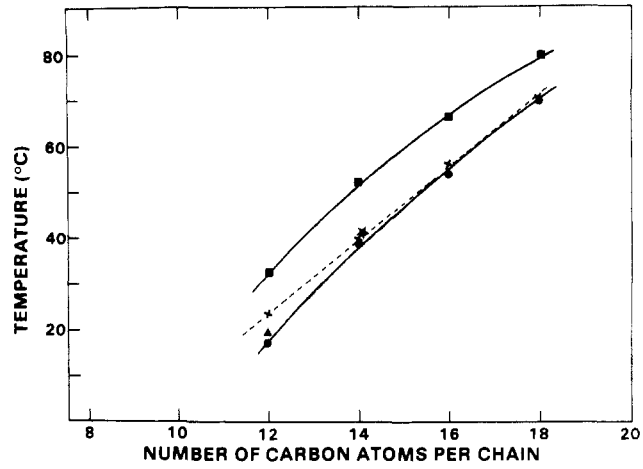

FIGURE 4: Transition temperatures (T_c) of hydrated diacylphosphatidylserines plotted as a function of the number of carbon atoms per hydrocarbon chain. (●) DL-DLPS (14 wt %), DMPS (21 wt %), DPPS (21 wt %), and DSPS (3 wt %) in 0.025 M ammonium phosphate buffer (pH 6.75, I = 0.05); (▲) DL-DLPS (15 wt %) in 0.25 M ammonium phosphate buffer (pH 6.75, I = 0.5); (★) DMPS (1 wt %) in 0.5 M ammonium phosphate buffer (pH 6.8); (×) ~50 wt % dispersions in 0.025 M ammonium phosphate buffer (pH 6.75, I = 0.05); (■) DL-DLPS (11 wt %), DMPS (21 wt %), DPPS (18 wt %), and DSPS (18 wt %) in 0.01 M HCl.

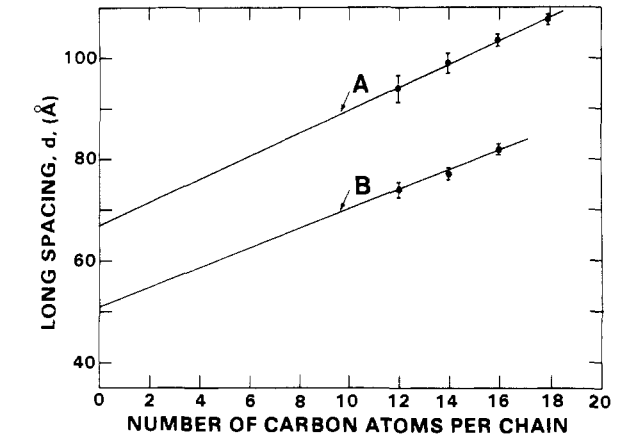

FIGURE 5: Lamellar repeat distance, d, of hydrated NH_4^+-PS at (A) temperatures below the gel → liquid-crystal transition temperature (T_c) and (B) temperatures above T_c. The data are presented as the mean ± SD and the solid lines represent the least-squares fit. NH_4^+-PS dispersions in 50 wt % 0.025 M ammonium phosphate buffer (pH 6.75, I = 0.05) were measured at 10 (DL-DLPS), 12 (DMPS and DPPS), and 20 °C (DSPS) in (A). In (B), DL-DLPS, DMPS, and DPPS were all recorded at 64 °C.

These extrapolated values correspond to the thickness of two polar-group layers plus the intercalated water thickness at 50 wt % water.

For NH_4^+-DSPS in the gel state, a typical lamellar phase d = 108 Å is observed (see Figure 5). However at 82 °C, above its thermotropic transition, a series of reflections (d = 93.7, 54.5, 47.1, and 26.6 Å) are observed for NH_4^+-DSPS, which index according to a hexagonal (presumably type II) phase. Thus, in contrast with the rest of the series (Figure 5), NH_4^+-DSPS appears not to form a lamellar phase at $T > T_c$, perhaps because the bilayer structure is not stable at the relatively high temperature of 82 °C.

Hydrated Dimyristoylphosphatidylserine. The effect of increasing hydration on the thermotropic behavior of the NH_4^+ salt of DMPS was studied by DSC. In the anhydrous state NH_4^+-DMPS undergoes a crystal → liquid-crystal transition at 70 °C. With increasing water content the reversible gel → liquid-crystal transition occurs at progressively lower tem-

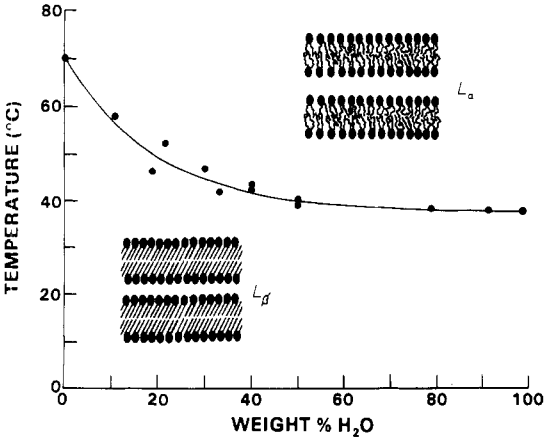

FIGURE 6: Transition temperature (T_c) of hydrated NH_4^+-DMPS as a function of water content. Transition temperatures were derived from the endotherm maxima of the DSC heating curves recorded at 5 °C/min. We have indicated that the hydrated gel of NH_4^+-DMPS has a small molecular tilt, i.e., $L_{\beta'}$ structure. Although this is suggested by the increment per CH_2 group (see Figure 5 and text), this is not conclusive. Thus, we cannot at this stage rule out the possibility that the hydrocarbons are perpendicular to the bilayer plane (L_β structure).

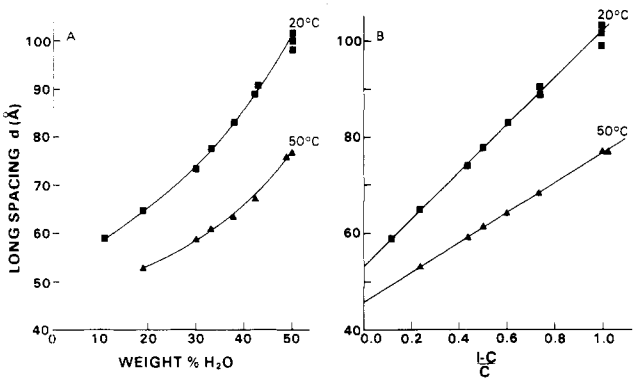

FIGURE 7: (A) Bilayer repeat distance, d, for hydrated NH_4^+-DMPS as a function of water content at 20 (■) and 50 °C (▲). The samples were dispersed in 0.025 M ammonium phosphate (pH 6.75, I = 0.05). (B) Bilayer repeat distance, d, for hydrated NH_4^+-DMPS plotted as a function of $(1 - c)/c$ where c is the concentration of lipid in wt fraction. The solid lines are least-squares fits to the experimental points. Extrapolation to $(1 - c)/c \rightarrow 0$ gives the thickness of the lipid bilayer.

peratures, reaching a limiting value of 39 °C at a water content of approximately 45 wt % (Figure 6). On the basis of this thermotropic behavior, X-ray diffraction studies of NH_4^+-DMPS were performed as a function of water content at temperatures below (20 °C) and above (50 °C) the gel → liquid-crystal transition. At 20 °C the wide-angle reflection at 1/4.2 $Å^{-1}$ confirms the presence at all water contents of the "hexagonal" hydrocarbon chain packing characteristic of the gel state. The lamellar bilayer repeat distance, d, increases continuously with increased water content up to at least 50 wt % water (Figure 7A). For continuous swelling lipid–water systems at high hydration levels, multilayer stacking disorders result in a broadening of the low-angle diffraction lines. This stacking disorder effect is observed for NH_4^+-DMPS for water contents ≥ 50 wt %. As shown in Figure 7B, the plot of d vs. $(1 - c)/c$ (where c is the concentration of lipid in weight fraction) is linear, indicating that the lipid bilayer structure does not undergo significant structural changes as a function of hydration. Extrapolation to $(1 - c)/c = 0$ yields the lipid bilayer thickness in the presence of water, and a value of 53 Å was derived for NH_4^+-DMPS at 20 °C. At 50 °C, the broad wide-angle reflection at 1/4.6 $Å^{-1}$ indicates that at water contents ≥ 20 wt %, the melted chain, liquid-crystal phase is

Table III: Bilayer Parameters of Hydrated NH_4^+-DMPS Derived from X-ray Electron Density Profiles

temp (°C)	wt % water	d (Å)	bilayer thickness[a] (P–P separation) (Å)	water thickness (Å)
20	19	65.5	44.0	21.5
20	30	73.5	45.0	28.5
20	33	78.0	46.0	32.0
20	38	83.4	44.0	39.4
20	50	101.1	45.0	56.1
50	30	38.7	41.0	17.7
50	42	67.3	42.0	25.3
50	50	77.2	41.0	36.2

[a] At 20 °C, mean value of bilayer thickness = 44.8 ± 0.8 Å. At 50 °C, mean value of bilayer thickness = 41.3 ± 0.6 Å.

present. Again continuous bilayer swelling occurs up to 50 wt % water, and no evidence of a hydration limit is observed (Figure 7A). The plot of d vs. $(1 - c)/c$ is linear and the derived lipid thickness corresponding to the liquid crystalline bilayer is 46 Å (Figure 7B).

For hydrated phospholipid systems, the Fourier transform of a single bilayer is sampled at specific points. A plot of the amplitude curve $|F|$ $(=|I^{1/2}|)$ vs. s $(=2 \sin \theta/\lambda)$ enables the regions in reciprocal space where the Fourier transform changes sign to be established. The corresponding Fourier transform curves $F(s)$ for NH_4^+-DMPS at 20 and 50 °C are shown in parts A and B of Figure 8, respectively. The transform curves allow all the diffraction patterns to be phased and the corresponding electron density profiles $\rho(x)$ to be calculated. The low-resolution electron density profiles of NH_4^+-DMPS bilayers at 20 and 50 °C are shown at different hydration levels in parts C and D of Figure 8, respectively. At 20 °C in the gel bilayer phase, it is clear that in the hydration range 19–50 wt % water, the peak to peak (PO_4–PO_4) separation across the bilayer remains constant at 44.8 ± 0.8 Å while the interbilayer aqueous space increases in thickness from 21.5 to 56.1 Å (see Figure 8C and Table III). Similarly at 50 °C in the liquid-crystal bilayer phase the PO_4–PO_4 separation across the bilayer is reduced, compared to the gel phase, to a value of 41.3 ± 0.6 Å (Figure 8D and Table III). This measure of the lipid bilayer thickness appears to be constant at hydration levels 30–50 wt % water (Table III). The interbilayer separation, a measure of the thickness of the aqueous space, increases from 17.7 to 36.2 Å over this hydration range (Table III). In contrast to the continuous hydration behavior exhibited by the NH_4^+ salts of PS, no significant change in the bilayer periodicity d was observed for acidic DMPS or acidic DPPS when dispersed in either 0.1 M HCl or water over the concentration range 19–92 wt % solvent.

Discussion

Low-angle X-ray diffraction data shown in Figure 1 indicate that anhydrous acidic PS exhibits two polymorphic crystal forms. Crystallization from either chloroform/methanol (2:1 v/v) or precipitation from chloroform solution with acetone usually produces the lamellar, presumably bilayer, crystal form I. A similar structural form is exhibited by the NH_4^+ salts and probably the K^+ salts of PS. The hydrocarbon chains are aligned approximately normal to the bilayer plane with little or no molecular tilt, a similar arrangement to that of phosphatidylethanolamine in the crystalline state (Hitchcock et al., 1974; Elder et al., 1977). The small value obtained for the thickness/polar group of approximately 6 Å suggests that the glycerophosphoserine has a gauche–gauche conformation

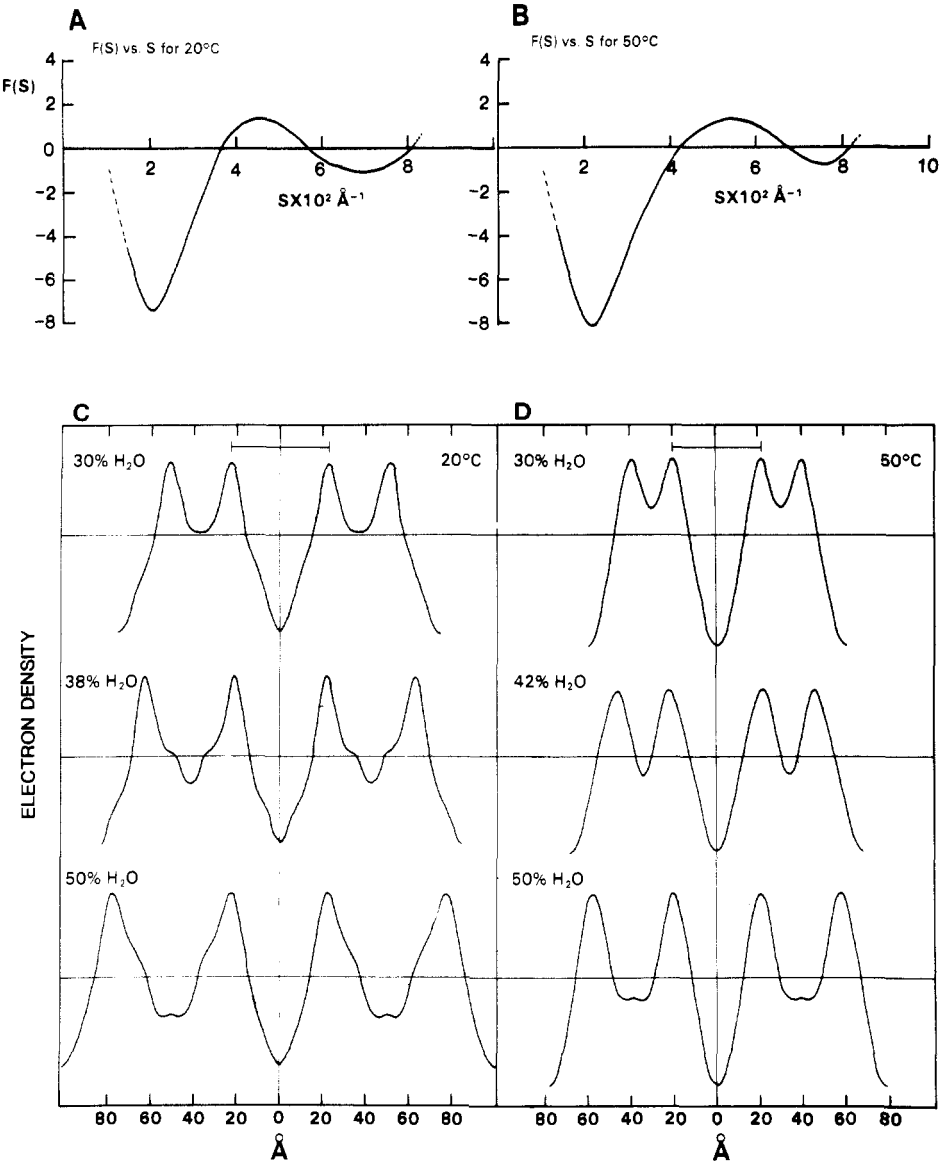

FIGURE 8: X-ray diffraction amplitude curves $F(s)$ for hydrated NH_4^+-DMPS at 20 (A) and 50 °C (B). Electron density profiles $\rho(x)$ for NH_4^+-DMPS containing 30, 38, and 50 wt % ammonium phosphate buffer at 20 °C are shown in (C). Electron density profiles for 30, 42, and 50 wt % dispersions at 50 °C are shown in (D). The ⊢⊣ indicates PO_4–PO_4 separation across a bilayer.

at the phosphodiester group such that the phosphoserine moiety lies parallel to the bilayer surface plane, as in the crystalline form of both phosphatidylethanolamine and phosphatidylcholine (Hauser et al., 1981). However, details of the PS conformation and packing arrangement await proper single-crystal analysis. In some cases the acidic PS (not the salts) crystallize in a different form (crystal form II) in which the hydrocarbon chains appear to be tilted with respect to the bilayer normal. For acidic DPPS, heating crystal form II to 125 °C followed by cooling to 30 °C produces crystal form I. This polymorphic form then undergoes reversible thermotropic behavior (see Figure 2). Above the hydrocarbon chain melting transition the low-angle diffraction lines index according to a hexagonal lattice $[1:(1/3^{1/2}):(1/4^{1/2})...]$. This would suggest the formation of the hexagonal H_{II} phase described by Luzzati (1968) with rod-shaped aggregates, the polar groups at the center of the rod and the fatty acid chains projecting to form the rod surface. The cylindrical rods pack in an hexagonal lattice.

Following an initial heating to above the crystal → liquid-crystal transition, the subsequent thermotropic behavior of anhydrous acidic PS and NH_4^+-PS is reversible and reproducible. The crystal → liquid-crystal transition temperature increases with increasing chain length, the transition of the NH_4^+ salts being systematically higher than that of the corresponding acidic PS. The transition enthalpies also increase with increasing chain length, but in this case the transition enthalpies of the acidic PS are systematically higher than those of the NH_4 salts. At the transition midpoint $\Delta G = 0$ and the entropy change at the transition $\Delta S = \Delta H/T$. The entropy change ΔS at the order–disorder transition is shown in Table I, and clearly ΔS [kcal/(mol·K)] of the acidic PS is almost twice that of the corresponding NH_4^+ salt. When ΔS is expressed per CH_2 group a value of 2.1 cal/CH_2·K is obtained for acidic PS and 3.24 cal/CH_2·K for the NH_4^+-PS salts. At present it is not possible to identify the structural basis of these pronounced differences in thermodynamic behavior, and more detailed structural studies of anhydrous PS are clearly warranted.

Differential scanning calorimetry of fully hydrated acidic PS and NH_4^+-PS shows reproducible and reversible gel → liquid crystalline transitions that are hydrocarbon chain length dependent. In this case the acidic form undergoes this transition at higher temperature but with a lower enthalpy change

than the NH_4^+ salt. When expressed in terms of CH_2 units, the entropy change for the NH_4^+ salts is 2.60 cal/CH_2·K, a somewhat smaller transition entropy change than for the acidic PS, 3.34 cal/CH_2·K. As would be expected, the thermotropic behavior of 50 wt % dispersions of NH_4^+-PS in buffer was similar to that of the more dilute dispersions (see Figure 4).

The X-ray diffraction data recorded for the series of 50 wt % NH_4^+-PS demonstrate that all members of this series show similar structural behavior below and above the order–disorder transition. The sharp 1/4.2 $Å^{-1}$ diffraction line observed at temperatures below the transition confirms the presence of an ordered gel phase with the hydrocarbon chains packed in a hexagonal lattice. Above the transition a broad diffraction line at 1/4.6 $Å^{-1}$ characteristic of the liquid-crystal phase is always observed. Both below and above the phase transition low-angle X-ray diffraction shows that only lamellar bilayer structures are present. The linear dependence of the bilayer repeat distance on chain length (Figure 5) suggests that the bilayer structure below the transition is similar for all members of the series. The increment per CH_2 group of 2.28 Å would suggest that the hydrocarbon chains are slightly tilted with respect to the bilayer normal, and with Luzzati's nomenclature (Luzzati, 1968) the NH_4^+-PS gel phase is denoted $L_{\beta'}$. At 50% water the combined thickness of the aqueous layer plus the thickness of two glycerophosphoserine groups is 67 Å for all members of the homologous series. Above the transition, again the linear dependence of d with chain length indicates similar structural arrangements in the liquid-crystal phase. This phase is a lamellar bilayer with the hydrocarbon chains in their melted configuration, L_α (Luzzati, 1968). The head group plus intercalated water thickness is reduced to 51 Å. This reduction is explained by the increase in surface area occupied by each PS molecule at the lipid–water interface, only the same amount of water is available to interact with the expanded PS surface. Thus, the water molecules reassemble to hydrate the increased surface area with the result that the thickness of the aqueous layer decreases, in this case by approximately 16 Å.

The combined DSC and X-ray diffraction study of the hydration of NH_4^+-DMPS results in the definition of the temperature–composition phase diagram. The thermotropic order–disorder chain melting transition temperature decreases with increasing hydration reaching a limiting value of 39 °C at approximately 45 wt % water. X-ray diffraction confirms the presence of a hydrated gel bilayer structure that takes up water continuously, a characteristic of lipid bilayers with a net charge (Atkinson et al., 1974). The hydrocarbon chains are packed in a hexagonal lattice, and there may be chain tilting with respect to the bilayer normal (see Figure 6). Above the chain melting transition only a lamellar lipid bilayer phase is observed, again with the property of continuous hydration. The bilayer structure in both the gel and liquid-crystal phases is confirmed by the electron density profile shown in Figure 8. The separation of the two electron dense peaks is a measure of the phosphorus–phosphorus separation across the bilayer, in turn a measure of bilayer thickness. At 20 °C the phosphorus–phosphorus distance is invariant at 44.8 Å over the hydration range 19–50 wt % water (see Table III). Over this hydration range the P–P separation across the aqueous layer, a measure of the water thickness, increases from ~22 to 56 Å. At 50 °C the bilayer thickness is again constant at 41.3 Å, and over the hydration range 30–50 wt % water, the water thickness increases from 18 to 36 Å. Thus, on going through the chain melting transition the bilayer thickness (P–P separation) decreases by 3.5 Å (44.8 to 41.3 Å) and the area/DMPS molecule at the lipid interface increases, resulting in a reduction of the aqueous thickness. At 50 wt % water, the reduction in aqueous layer thickness of ~20 Å is somewhat higher than that estimated from the homologous series, ~16 Å (see above and Figure 5). Thus, for the NH_4^+-DMPS/water system, the binary phase diagram in the temperature range 0–70 °C consists of two single-phase zones: at low temperatures, a continuously expanding bilayer $L_{\beta'}$ gel phase and above the chain melting transition a continuously expanding bilayer L_α liquid-crystal phase (Figure 6).

These studies have provided detailed structural and thermodynamic information on the acidic and NH_4^+ salt forms of a homologous series of diacyl-PS. These structural and thermodynamic parameters are essential for understanding the changes in PS bilayer membrane properties induced by monovalent (Li^+, Na^+, K^+, and Rb^+) and divalent (Ca^{2+} and Mg^{2+}) cations (H. Hauser and G. G. Shipley, unpublished results).

Added in Proof

A recent study utilizing ESR spin labeling and DSC provides additional information on the pH, NaCl, and hydration dependence of the thermotropic transitions of DMPS and DPPS (Cevc et al., 1981).

References

Aneja, R., Chadha, J. S., & Davies, A. P. (1970) *Biochim. Biophys. Acta 218*, 102–111.

Atkinson, D., Hauser, H., Shipley, G. G., & Stubbs, J. M. (1974) *Biochim. Biophys. Acta 339*, 10–29.

Browning, J. L., & Seelig, J. (1980) *Biochemistry 19*, 1262–1270.

Cecv, G., Watts, A., & Marsh, D. (1981) *Biochemistry 20*, 4955–4965.

Elder, M., Hitchcock, P., Mason, R., & Shipley, G. G. (1977) *Proc. R. Soc. London, Ser. A 354*, 157–170.

Elliott, A. J. (1965) *J. Sci. Instrum. 42*, 312–316.

Hauser, H., & Phillips, M. C. (1979) *Prog. Surf. Membr. Sci. 13*, 297–413.

Hauser, H., Pascher, I., Pearson, R. H., & Sundell, S. (1981) *Biochim. Biophys. Acta 650*, 21–51.

Hitchcock, P. B., Mason, R., Thomas, K. M., & Shipley, G. G. (1974) *Proc. Natl. Acad. Sci. U.S.A. 71*, 3036–3040.

Janiak, M. J., Small, D. M., & Shipley, G. G. (1976) *Biochemistry 15*, 4575–4580.

Kates, M. (1975) *Techniques of Lipidology*, pp 444–446, North-Holland, Amsterdam and Oxford.

Luna, E., & McConnell, H. M. (1977) *Biochim. Biophys. Acta 470*, 303–316.

Luzzati, V. (1968) *Biol. Membr. 1*, 71–123.

MacDonald, R. C., Simon, S. A., & Baer, E. (1976) *Biochemistry 15*, 885–891.

Papahadjopoulos, D., Vail, W. J., Newton, C., Nir, S., Jacobson, K., Poste, G., & Lazo, R. (1977) *Biochim. Biophys. Acta 465*, 579–598.

Shipley, G. G. (1973) *Biol. Membr. 2*, 1–89.

van Dijck, P. W. M. (1979) *Biochim. Biophys. Acta 555*, 89–101.

van Dijck, P. W. M., de Kruijff, B., Verkleij, A. J., van Deenen, L. L. M., & deGier, J. (1978) *Biochim. Biophys. Acta 512*, 84–96.